Understanding the dynamic of POMS infection and the role of microbiota composition in the survival of Pacific oysters, Crassostrea gigas.

Lizenn Delisle (lizenn.delisle@Cawthron.org.nz)
Cawthron Institute
Olivier Laroche
Cawthron Institute
Zoë Hilton
Cawthron Institute
Jean-François Burguin
Cawthron Institute
Anne Rolton
Cawthron Institute
Jolene Berry
Cawthron Institute
Xavier Pochon
Cawthron Institute
Pierre Boudry
French Research Institute for Exploitation of the Sea
Julien Vignier
Cawthron Institute

Research Article

Keywords: OsHV-1, oyster, POMS, microbiome, 16S rRNA gene sequencing, Droplet digital PCR

Posted Date: June 6th, 2022

DOI: https://doi.org/10.21203/rs.3.rs-1636731/v1

Abstract

Background:

In recent years, the aquaculture industry of *Crassostrea gigas* has been severely impacted by geographically widespread outbreaks of a polymicrobial disease, the Pacific Oyster Mortality Syndrome (POMS). The aetiology of these recurring summer mortality events and the disease progression have notably been recently described in France, revealing a combined development of viral (namely the Ostreid Herpesvirus, OsHV-1 µVar) and bacterial infections. In New Zealand (NZ), mass mortality episodes associated with OsHV-1 have been recorded in juvenile *C. gigas* since 2010 and selective breeding to improve resistance to OsHV-1 has been effectively used to mitigate the impact of the disease. However, POMS infection process and the role of the host-microbiota during infection have still not been well established in NZ.

Results:

Using a laboratory-based experimental infection approach, we challenged ten biparental oyster families with previously established contrasted genetically based ability to survive POMS in the field. Molecular analyses (viral load quantification, viral gene expression and 16S rRNA gene sequencing) were combined with histopathological observations to describe the temporal kinetics of infection to POMS and to characterize the role of microbiota during infection. Our main findings showed (1) a delay in viral infection resulting in a late onset of mortality in oysters compared to previous observations from France, and (2) a lack of evidence of major fatal bacteraemia in infected oysters. Bacterial profiling associated the microbiota composition with mortality rate, viral load, and viral replication, allowing the identification of potentially deleterious and beneficial bacterial taxa that can influence the outcome of the disease. *Mycoplasma* ASV-1 was identified as a significant predictor of mortality in oysters.

Conclusion:

Collectively, these results could improve current disease management and aquaculture practices and help understanding the mechanisms behind genetic resistance to POMS. Ultimately, microbiome composition could be used to predict oyster mortality following exposure to OsHV-1 and be used as a complementary screening tool in selective breeding and/or a diagnostic tool to determine shellfish health.

1. Background

Over the last decade, the Pacific Oyster Mortality Syndrome (POMS) has been the major challenge for the growth of Pacific oyster in most production countries. Since 2008, recurrent mass mortality events associated with OsHV-1 *µ*Var have been recorded in numerous countries producing *Crassostrea gigas*, inducing 40 to 100% mortality in less than one year old oysters [1–3]. The first major outbreak was recorded in France during the summer of 2008 [4]. The same year, OsHV-1 µVar was detected along the

European coastline from southern Norway to Portugal [3, 5] and closely related variants were detected during massive mortality events in Australia [6] New Zealand [7] Korea [8] and more recently California [9].

The POMS is a polymicrobial disease caused by the combined development of viral and bacterial infections [10]. Disease occurrence is multifactorial and depends on multiple factors influencing the host, the pathogens and the environment. Among those, biological factors such as genetic background and developmental stage [11–14], metabolism and diet [15] and environmental factors, mainly the water temperature [16–18], are the most prominent. Experimental challenges using oyster families with contrasted resistance to OsHV-1 recently led to a better understanding of the POMS infection process. Twelve hours after exposing the vulnerable oysters to OsHV-1 µVar, an intense viral replication is detected. At 48h, the viral load and the transcriptional activity are maximal and remain stable until the first death at 66 hours post infection in vulnerable oysters. The viral gene expression induces an immune-compromised state that concomitantly allows for a massive colonization of the gills by opportunistic bacteria evolving towards a bacteraemia and leading to oyster death [10]. In contrast, resistant oysters (i.e., which commonly experience very low mortality, less than 5%), weakly replicate OsHV-1 and do not show changes in their microbiota composition after being exposed to a high viral load [10, 14].

The role of the oyster microbiota in POMS is complex and ambivalent. For instance, microbiota composition is highly variable in relation to geographic location, seasonality, oyster age, tissue type and health status [19–23]. Changes in at least one of these parameters associated with an immune-compromised state in oysters can influence disease occurrence by inducing the replacement of benign microbial colonizers with a consortium of different pathogens [22]. Administering antibiotic treatment early after OsHV-1 infection was shown to reduce mortality compared to untreated oysters, underlying the key role of bacteria in the pathogenicity of the disease [10]. It has been demonstrated that an increase in bacterial load, mainly in the *Vibrio* community, is necessary to cause mortality during POMS [23–25]. Moreover, recent studies showed significant differences in the structure of the microbiome of oysters exhibiting various levels of susceptibility to POMS [19, 26]. For example, the genera *Arcobacter*, *Marinomonas*, *Psychrobium*, *Psychromonas* and *Vibrio* were identified as direct contributors to the bacteraemia after viral burst [10, 19, 24, 26]. Some evidence also suggest that microbiota might protect the host from pathogens [27], acting as a physical barrier by producing antimicrobial peptides [28, 29] or stimulating the immunity of their host [30, 31].

In New Zealand, the presence of a herpes-like virus was first reported in 1992 after massive mortality of 7-day old *C. gigas* larvae occurred in a hatchery [32]. However, it was not until April 2010 that the first massive mortalities affecting juvenile oysters were observed, where multiple oyster translocations led to a fast spread nation-wide. The OsHV-1 variant (JN639858) identified in oysters during the 2010 outbreak presented typical µvar deletions in the C2-C6 region (ORF 4) but also shared two identical nucleotides with the reference strain (AY509253), that differed from the variant µvar (HQ842610,[7]).

Little is known about the POMS infection process in New Zealand. A field study carried out in the summer of 2010-11 recorded 14% spat mortality after 6 days of deployment on aquaculture farms, increasing to

50% after 9 days and 70% after 13 days - a relatively late dynamic of infection - with an increase in viral load and *Vibrio* detected in oysters after 4 days [7]. These field-based observations suggest that further knowledge of the dynamics of POMS infection is necessary to improve POMS risk management, but also to support the New Zealand oyster aquaculture industry and to sustain the development of new mitigation strategies in New Zealand.

In the present study, we primarily aimed to (i) describe the POMS infection process in New Zealand and (ii) characterize the temporal dynamics of the microbiota associated with oysters after exposure to a purified isolate of OsHV-1. We used a lab-based experimental infection approach, that reproduces the natural route of infection, to challenge ten biparental oyster families displaying contrasted genetically based susceptibility to the POMS, combined with various molecular analyses (viral load quantification, viral gene expression and 16S rRNA gene sequencing) and histopathological assessments to describe the kinetics of infection to POMS.

2. Methods

2.1 Pacific oyster family production and maintenance

Ten biparental Pacific oyster (*Crassostrea gigas*) families were produced in March 2019 at the Cawthron Institute's hatchery in Nelson, New Zealand (41°11'33.3"S, 173°21'37.8"E). Broodstock selected for spawning originated from the Mahurangi harbour (Warkworth, New-Zealand; 36°25'28.16"S, 174°41'32.36"E). Parents used to produce resilient families have been selected for three generations and were survivors from full-sib families that had been exposed to an on-farm virus challenge and selected based on their high survival rates in the field. Parents used to produce susceptible families were derived from i) a subset of the families that showed poor survival during the on-farm challenge; and ii) specific males that were reared on an uninfected farm on the South Island, and were, therefore, expected to be naïve and highly susceptible to the virus [12]. Cryopreserved sperm from these individual naïve males were thawed according to Adams et al. [33].

Twenty million eggs from each female were fertilized with either fresh sperm or thawed sperm from a single male. Resulting embryos from a single cross were then incubated separately for 24h according to [34]. Individual families were reared using a high-density larval rearing flow-through system in the hatchery for 5 weeks according to a modified protocol from Ragg et al. [35] .

Oyster families were then further on-grown for 5 months in a common flow-through water tank but kept separate in family-specific upwelling tanks. All families were reared under common conditions: seawater temperature ranged from 9°C to 18°C, and algal food was continuously supplied to provide an optimal growing environment for the spat. Husbandry treatments such as grading and biomass adjustments, were conducted simultaneously between families. Despite these measures, mean liveweight of spat at the beginning of the trial varied among families (Supplementary Table 1). In the nursery tank, oyster families were continuously supplied with UV-sterilized seawater (80 mJ cm^{-2}) and maintained under strict

biosecurity management to ensure that no pathogen would interfere with later experiments. The "pathogen free" status of the experimental oysters was confirmed prior to the initiation of the experiment: indeed, no OsHV-1 DNA was detected using qPCR (n=100; [36]). Finally, no significant spat mortality was observed prior to the start of the experiment.

2.2. Experimental design

2.2.1. Acclimation of oysters

On the 4th September 2019, virus-free oysters were randomly collected from their family-specific upwelling tanks and transferred to the experimental challenge facility at the Cawthron Institute (Nelson, New-Zealand; 41°16'16.7"S, 173°17'36.3"E) for acclimation.

Experimental infection protocols consisted of a water transfer between tanks containing *C. gigas* oysters carrying the disease (referred as 'donors') and tanks containing pathogen-free oysters (referred as 'recipients') adapted from [16,18,37]. Two pools of 5,000 spat each (6-month-old oysters, mean individual weight of ~ 1.2 g), consisting of a mixture of oysters from our susceptible families, were used as "donors", and placed in two 300L tanks; one tank for the control donors (which were to be injected with artificial seawater) and one tank for the pathogen donors (which were to be injected with OsHV-1 suspension) (Fig. 1). Tanks were continuously supplied with 1 µm-filtered and UV-sterilized seawater (FSW), preheated through a Digiheat inline heater (Waterco, Auckland, New Zealand), and flow rates were maintained at 1.5L min^{-1} per tank. Donors were maintained in these conditions for 2 weeks until their injection.

In parallel, family-specific mesh bags containing 195 oysters (6-month-old spat, mean individual weight of ~ 1.2 g) were prepared for each of the 10 families and used as "recipients". One bag per family was randomly suspended (i.e., 10 families x 1 bag = 10 bags per tank) into six 100L tanks. Three replicate recipient tanks were set up for the pathogen group and three replicates for the control group (Fig. 1 A, B). Total biomass per recipient tank (corresponding to 1,950 spat) was 2.4 kg ± 0.2. Flow rates were adjusted to 0.5L min^{-1} for each tank by means of a valve so combined flow rate for the triplicate tanks was 1.5L min^{-1}. Recipient oysters were acclimated under these conditions for 15 days until viral inoculation. No mortality was observed during this time.

To thoroughly maintain seawater temperature at 20.8°C (± 0.8), oxygen saturation above 90% and seawater well homogenized, all tanks were equipped with an aquarium immersion heater (Eheim thermocontrol 200W), light aeration, and a circulation pump (Hailea, Low water level pump DS-700). All oysters (donors and recipients) were fed *ad libitum* with a bispecific mixture of hatchery-grown *Chaetoceros muelleri* (CS-176) and *Tisochrysis lutea* (CS-177) continuously supplied using a peristaltic pump. Algal background concentration was maintained between 3 to 10 µg L-1 Chlα (equivalent to 5 to 20 cells of *Tiso* per µL).

2.2.2 Viral suspension

The OsHV-1 suspension stock was produced in April 2014 as described in Camara et al. [12]. Briefly, tissue from high virus load oysters was homogenized, cell debris was removed by centrifugation, and the supernatant was purified by serial filtrations to 0.22 µm. Finally, a cryoprotectant solution (10% glycerol and 10% fetal calf serum final concentration) was added and the resulting suspension slowly frozen and stored at −80 °C.

2.2.3 Infection and sampling procedures

On the 17th September 2019, pathogen-donor oysters were myorelaxed in hexahydrate $MgCl_2$ (30 g L^{-1}) according to [38] until valve opening. Concurrently, cryopreserved virus stock suspension was thawed in a 22°C water bath for 10 minutes, and diluted 1/5 in sterile artificial seawater (SSW). Pathogen donors were then injected in the adductor muscle using a 26-gauge needle attached to a multi-dispensing hand pipette, with 20 µl of viral suspension (1.76 x 10^5 copies of OsHV-1 per injection), while “control donors” were injected with the same volume of sterile SSW. Oyster donors (pathogen and control) were then held at 22°C (± 0.5) for 70 h in their respective tanks, in static conditions (i.e., no water renewal) to produce infectious or control water. During the incubation period, survival of donor oysters was monitored daily, and dead animals were immediately removed from the tanks.

On the 20th September, infectious or control water was transferred to the respective recipient tanks (3 tanks OsHV-1 challenged, 3 tanks control). Feeding was stopped and the recipient tanks were left in static conditions at 22°C (± 0.5). After 48 hours, new FSW was gradually reintroduced to the recipient tanks at a flow rate of 0.5 L min^{-1}. Recipients were then inspected daily and dead animals, characterized by failure to close their valves, were immediately removed. Survival of recipients was monitored for 14 days or 336 hours post infection (hpi). To avoid accidental releases of OsHV-1 in the environment, continuous chlorination (200 ppm for 1h) combined with UV sterilization (80 mJ cm^{-2}) were applied to the effluent water.

Five live recipient oysters were randomly sampled from each family-specific bag at 0, 2, 6, 12, 24 hpi, and every 24h until 120 hpi. A final sampling of 5 live recipient oysters was conducted at the end of the challenge, at 336 hpi (Fig. 1). Whole tissues were removed from the shells, dried by dabbing on a paper tissue, flash frozen in liquid nitrogen and later reduced to powder (Mixer Mill MM400, Retsch GmbH, Germany) and stored at -80°C for OsHV-1 DNA, viral gene expression and metabarcoding analyses. In addition, three live recipients were randomly collected from each family-specific bag at 0 and 72 hpi. Their tissues were carefully dissected, placed in histological cassettes, fixed in 4% formalin for 48h and stored in 70% ethanol for later histopathological analysis.

One liter of seawater was collected from each donor tank (n = 2) at 0, 48 and 72 hpi, while 1L of seawater from each recipient tank (n = 6) was sampled at 0, 24, 48, 72, 96, 120, 168, 240, and 288 hpi (Fig. 1). Water was collected using sterile (autoclaved) glass bottles, and immediately filtered through a sterile 47 mm cellulose membrane filter of 0.22 µm pore size to isolate bacteria and viruses. Membrane filters were flash frozen and stored at -80°C until DNA extraction.

2.3 Biometric analyses and water quality measurements

Each family-specific mesh bag was weighed on the 4th of September prior to acclimation (ST 1), on T_0 (prior to viral infection), and at the end of the challenge on the 4th of October (T_{336h}).

Water quality parameters were measured throughout the challenge by means of a YSI ProSolo digital meter (Xylem Inc., Yellow Springs, OH, USA) for temperature and dissolved oxygen (D.O), a handheld Testo 206 pH meter for pH, and a FluoroSense handheld fluorometer (Turner Designs, San Jose, CA, USA) for microalgal background levels.

2.4 DNA extraction and OsHV-1 DNA quantification

Total DNA was extracted from powdered donors (0 hpi) and recipient oysters (0 and 120 hpi), and from seawater samples from donor tanks (0, 48 and 72 hpi) and recipient tanks (0, 24, 48, 72, 96, 120, 168, 240, 288, 336 hpi) using Blood and tissues kit (QIAGEN) according to the manufacturer's protocol. Four blank DNA extractions were included in order to test for potential bacterial contamination of the DNA extraction kit and/or reagents.

Level of OsHV-1 DNA was quantified using real time PCR in water from both donors (0, 48 and 72 hpi) and recipient tanks (0, 24, 48, 72, 96, 120, 168, 240 hpi) (Fig. 1). Real time PCR was carried out in 20 µl reaction mixture consisting of 10 µl of SsoFast Tm EvaGreen Supermix (Biorad), 1 µl of each primer (OsHV-1 BF and OsHV-1 B4, 10 µM), 6 µl of water and 2 µl DNA sample. PCR amplification was performed using Rotor-Gene R Q (Qiagen) following: 1 cycle pre-incubation at 98°C for 2 min, 40 cycles of amplification at 98°C for 15 s and 58°C for 20 s; melting temperature curve Ramping from 72°C to 95°C, rising by 1 degree each 5 second. Samples were analysed in triplicate, and 3 controls were carried out: a negative control which contained PCR reaction mixture without the target, an extraction control and a positive control which holds DNA target(s). The standard curve was prepared using serial dilutions of chromosomal DNA from Sydney University (Sydney School of Veterinary Science, Infectious Disease Laboratory, Farm Animal Health, Australia), to determine OsHV-1 DNA concentration.

2.5 Microbiota sequencing

Polymerase chain reactions (PCR) were performed on some of the samples extracted as described earlier (n = 120 from oyster tissue.; n = 54 from water, plus blank controls). Bacterial communities were amplified using the 16S rRNA gene (v3-v4 region) with the primer set 341F: 5'-CCT ACG GGN GGC WGC AG-3'[39] and 805R: 5'-GAC TAC HVG GGT ATC TAA TCC-3' [40]. These primers were modified to include Illumina^{TM} overhang adaptors (forward: 5'-TCG TCG GCA GCG TCA GAT GTG TAT AAG AGA CAG-3' and reverse: 5'- GTC TCG TGG GCT CGG AGA TGT GTA TAA GAG ACA G-3'), as described in Kozich et al. [41].

Polymerase chain reactions were carried out in 50 µL reaction volumes containing 25 µL MyFi^{TM} 2× PCR supermix (Bioline, London, UK), 19 µL of nuclease-free H20, 0.20 µM of modified Illumina overhang adaptor primers, 2.0 µM of both blocking primers, and 1 µL of template DNA. Thermocycling conditions

were 95°C for 2 min, followed by 39 cycles of 94°C for 20 s, 52°C for 20 s, 72°C for 30s, with a final extension step at 72°C for 5 min. Amplicons were purified using the SequalPrep^{TM} normalization plate kit (Applied Biosystems, CA, USA) resulting in an equimolar concentration of ~1 ng μL^{-1}, all according to the manufacturer's instructions. Purified amplicons were individually indexed using the Nextera^{TM} DNA library Prep Kit (Illumina, California, USA) and paired end sequenced on a MiSeq^{TM} Illumina with the 2x250 bp v2 kit at Auckland Genomics (Auckland, New-Zealand). Raw sequences are publicly available from the NCBI database under project number PRJNA832870.

2.6 Viral gene expression

Viral gene expression was quantified in recipient oysters from the ten families sampled at 6, 12, 24, 48, 96 and 120 hpi. RNA was extracted from 30 mg of powdered oysters using the Direct-Zol RNA Miniprep kit (Zymo research) according to the manufacturer's protocol. Samples were then treated with DNAse I (TURBO^{TM} DNase, Invitrogen) to remove genomic DNA. To confirm the absence of DNA in the sampled RNA, a 16S PCR assay was performed on each RNA sample after DNase treatment and gels were run. The quality and purity of the isolated RNA in all samples were checked using a NanoPhotometer (Implen, Munich, Germany). DNAse-treated RNA was transcribed into cDNA, using the Super-Script III reverse transcriptase (Life Technologies, CA, USA). Droplet digital PCR (ddPCR) was conducted in an automated droplet generator (QX200 Droplet Digital PCR System^{TM}, BioRad) to determine the expression of three viral genes ORF 27, ORF 38 and ORF 87 selected from among the 39 ORFs described by Segarra et al. [42]. These ORFs encode for different protein functions and expressed differently during an OsHV-1 replication cycle [42]. Each ddPCR reaction included 1 µl of 3 µM of each primer, 10 µl ddPCR Supermix for Evagreen (BioRad), 1 µl DNA and 7 µl sterile water for a total reaction volume of 21 µl. The BioRad QX200 droplet generator partitioned each reaction mixture into nano droplets by combining 20 µl of the reaction mixture with 70 µl of BioRad droplet oil. After processing, this resulted in a total nanodroplet volume of 40 µl, which was transferred to a PCR plate for amplification using the following cycling protocol: hold at 95°C for 5 s, 45 cycles of 95°C for 30 s, 60°C 1 s, and a final enzyme deactivation step at 98°C for 10 min. The plate was then analysed on the QX200 instrument. For each ddPCR plate run, at least one negative control (RNA/DNA-free water; Life Technologies), and one positive control (Gblock for each ORF tested, diluted 1/10,000) were included.

2.7 Histological analyses

Recipient oysters were collected for histopathological analysis at 0 and 72 hpi. Three individuals per family (10 families at 0 and exposed oysters at 72hpi and 3 families for non-exposed oysters at 72hpi) were sampled per tank (3 tanks). Following storage in 70% ethanol, whole oysters were embedded in paraffin wax, before being serially sectioned to a thickness of 5 µm using a microtome. Tissue sections were collected on polylysine-coated slides and stained with Giemsa (performed by Gribbles Veterinary pathology, New Zealand), which contains a mixture of azure and eosin that variably stain the basic components of the cell pink/purple (e.g cytoplasm, granules) and methylene blue, which stains the acidic components of the cells blue (e.g nucleus). The presence of histopathological features was assessed in

the mantle and digestive gland of oysters using a light microscope and up to 1000X magnification (Olympus BX53 microscope with a DP22 digital camera). Pathological features were categorised as '0' when absent and '1' when present and were converted to a percent presence of a given feature per family, keeping tank replication (n=3).

2.8 Bioinformatic analysis

Sequence data was demultiplexed using the MiSeq Reporter (v.2) and primers removed using CUTADAPT (Version 2.6; [43]) allowing for no indels and a minimum overlap of 17 base-pairs (bp). Sequences were quality filtered (maxN=0, maxEE=c(2,2), trunQ=2), denoised, paired end merged (minOverlap=10) and chimera filtered (method=consensus) using the 'DADA2' R program (version 1.14; [44]). Prior to quality filtering, forward and reverse reads were truncated at 226 and 220 bp on the 5' end, respectively, to remove the lower quality section. Amplicon sequence variants (ASVs) were taxonomically identified using the RDP Naïve Bayesian Classifier algorithm [45] (implemented in DADA2 using the SILVA ribosomal RNA gene database ([46]; version 138; https://benjjneb.github.io/dada2/training.html). Unassigned ASVs and those identified as non-bacterial were discarded. Additionally, potential contaminant reads were identified and removed with the MicroDecon R package ([47]; version 1.0.2) rare ASVs (ASVs for which the sum of read did not exceed more than 2 reads in at least 3 samples) were discarded. Sequencing depth per sample was visualized with the "rarecurve" function of the "vegan" R package (version 2.5.7; [48]), and samples with less than 10,000 reads discarded to ensure that samples used in downstream analyses had sufficient sequencing depth to recover most of the diversity.

2.9 Statistical analyses

Survival functions were computed according to Kaplan and Meier (1958) using RStudio 4.1.0 and the "Survival" R package (V 3.2-13, [49]). Survival time was measured in hours from the injection for (i) donors (Supplementary Data 1) or (ii) from the onset of infection for the recipients (Fig. 2). The data were read as the number of dead oysters within each bag per tank at each count. Survival time curves were compared using the cox regression model [50] after adjusting for (i) injection (OsHV-1 or SSW) for donors, or (ii) for family (F1 to F10), and infection level (OsHV-1 or control) for recipient oysters, considering the random effect of the tanks and bags. The survival of control recipient oysters was not included in the statistical model because it was 100%. The proportionality of hazards (PH) was checked based on Schoenfeld residuals [51].

Mixed-design, time-repeated ANOVAs were performed to assess differences in (i) OsHV-1 DNA load in water of recipient tanks according to Family (ten levels) and time (eight levels) and ii) percent presence of a pathological feature depending on family, time, and exposure to OsHV-1. The replication unit was the tank in which the ten families were maintained. All mutual interactions among factors were tested, and Tukey's honestly significant difference test was used as a post-hoc test. The normality of residuals and homogeneity of variances were graphically checked. Statistical analyses were performed in R studio, version 4.1.0 (R; https://www.R-project.org/). For viral gene expression, heatmaps were constructed using Multiple Experiment Viewer software ([52] http://mev.tm4.org/#/datasets/upload).

Microbial taxonomic composition in seawater and in oysters was investigated and visualised at phylum and family levels using bar plots and the 'ggplot2' R package (version 3.3.5; [53]). Alpha-diversity metrics such as ASV richness, Shannon and Simpson indexes were computed with the 'Phyloseq' R package (version 1.34.0; [54]) and visualised with line plots using 'ggplot2'. The effect of treatment, family type (vulnerable vs resistant vs highly resistant), collection date and their interactions on alpha-diversity metrics of oyster microbiota was investigated with linear mixed-effects regressions (LMER) using the 'lme4' R package (version 1.1.27; [55]). Similarly, the effect of treatment, time after start of experiment, and their interactions, on alpha-diversity metrics of seawater microbial communities was investigated with a LMER.

The effect of treatment on the oyster microbial community composition and structure was visualised with a principal component analysis (PCA) and tested with a permutational analysis of variance (PERMANOVA) using the 'vegan' R package (version 2.5.7; [48]) with the following parameters: adonis2 (Bray-Curtis distance matrix of read abundance table transformed to relative abundance ~ infection* family type + Time * family type, blocks = tank, permutations = 999, method = "bray", by = "terms"). Differences in core oyster microbiome between vulnerable and highly resistant families were investigated with heatmaps using the plot core function of the 'microbiome' R package (version 1.13.8; [56]) and using the 'ComplexHeatmap' R package (version 2.6.2;[57]).

Oyster bacterial genera associated with oyster mortality rate, ORF and viral load were investigated with Pearson correlation based on centered-log ratio transformed read abundance to account for the compositional nature of the data and visualised with a heatmap using the 'ggcorrplot' R package (version 0.1.3; [58]). In addition, interactions between these bacteria were assessed with the CoNet Cytoscape plugin (version 1.1.1; [59]) using Pearson correlations and the Bonferroni multiple-test correction. Variables that could best predict mortality rate, including oyster bacteria ASVs transformed to centered-log ratio, viral load and ORF concentration were identified using a Random Forest model trained (parameters: trControl = "repeatedcv", number = 5, repeats = 3, search="grid"; tunegrid = expand.grid(.try=c(1:8))) using the 'caret' R package (version 6.0.88; [60]) and visualised with bar plots using ggplot2.

3 Results

3.1 Survival and viral progression

Survival of pathogen donors (oysters injected with OsHV-1 suspension) was significantly reduced at 48h post injection and reached 29% at 72 hpi. By then, pathogen donors shed 2.64 x 10^9 OsHV-1 DNA copies per liter of surrounding seawater (Figure S1).

Survival of control recipient oysters was 100% irrespective of the family (Fig. 2). Very low levels of virus were observed in the control water samples (<1.10^2 OsHV-1 DNA copies per liter), likely the result of aerosolization of viral DNA during inoculation of OsHV-1 or during experimental handling. Because no

virus was amplified from tissue of control recipient oysters and no control recipient died, only the pathogen-exposed recipient oysters will be considered hereafter.

Mortality started 48 hpi. Specifically, significant mortalities (> 10 %) were recorded 144 hpi in Family 4 (F4), 168 hpi (F10), 192 hpi (F6, F7, F8, F9), 240 hpi (F5 and F3) whereas very low mortality (<10%) was observed for F1 and F2 (Figure 2). At the end of the experiment (336 hpi), the final survival of pathogen-exposed recipient oysters ranked as follow: F1 (99.3 % ± 0.4), F2 (92.8 % ± 1.1), F3 (82.0 % ± 2.3), F4 (76.8 % ± 2.1), F5 (73.8 % ± 2.2), F6 (71 % ± 2.2), F7 (70.2 % ± 2.3), F8 (68.5 % ± 2.3), F9 (58.9 % ± 2.4), F10 (50.8 % ± 2.5) (Figure 2).

Based on this final survival, F1 and F2 were subsequently grouped and classified as “highly resistant”, F3, F4, F5, F6, F7, and F8 as “resistant”, and F9 and F10 as “vulnerable”, this classification (Family type) will be used throughout.

At the onset of the experiment (i.e., prior to the transfer of infected waters), OsHV-1 DNA was not detected in the water from the recipient tanks (Table 1). Following infection, viral load in the water increased to reach 4.75×10^9 ($\pm 0.69 \times 10^9$) copies. L^{-1} at 168 hpi. By 240 hpi, viral load decreased to 2.05×10^7 ($\pm 1.44 \times 10^7$) copies. L^{-1} of water (Table 1). No significant differences were found in viral load between tanks over time ($p = 0.709$).

Table 1. Quantification of OsHV-1 DNA in recipient oysters.

Time (hpi)	OsHV-1 in water (copies. L^{-1})	*
0	0.00±0.0	c
24	$(3.87 \pm 1.2) \times 10^9$	a
48	$(2.92 \pm 1.68) \times 10^8$	a
72	$(6.65 \pm 2.08) \times 10^8$	a
96	$(7.96 \pm 3.34) \times 10^8$	a
120	$(5.41 \pm 1.11) \times 10^8$	a
168	$(4.75 \pm 0.69.) \times 10^9$	a
240	$(2.05 \pm 1.44) \times 10^7$	b

Quantity of viral DNA measured in the water of infected recipient tanks (n = 3). Data are expressed as copies of OsHV-1 per liter. Viral load was estimated before infection (0 hpi) and throughout. Hpi = hours post-infection. Different letters indicate statistical difference ($p \leq 0.05$) between timepoints.

Expression of the three OsHV-1 viral open reading frames (ORFs) were modulated as a function of the ORF, families and time. Specifically, ORF 38 was expressed in all families from 96 hpi with low expression levels in F1 and F10 (Figure 3). The ORFs 27 and 87 were also expressed in most families, except for families F2 and F5 where viral gene expression (viral replication) started at 120 hpi, and for F1 where ORF expression was never recorded (Figure 3). Family 8 exhibited the highest viral replication, whereas ORF expression associated with F1, F7 and F10 remained the lowest over time, suggesting very little viral replication occurred in these family lines.

3.2 Histological analyses

Significant differences ($p<0.05$) in the prevalence of pathological features were observed in the mantle and digestive gland between oyster spat exposed and not-exposed to OsHV-1 for 72h (Figures 4 and 5). Oysters exposed to OsHV-1 showed higher instances of 'loose' connective tissue (CT) in the mantle ($p= 0.0176$, nested ANOVA) and digestive gland ($p= 0.000147$, Figure 4A) compared with controls. This 'loose' CT tissue showed a loss of structure and large edematous areas (Figure 5B) compared to normal CT (Figure 5A). Significant differences in the occurrence of loose CT in the mantle were also observed between families ($p=0.0122$) and there were interactive effects of infection and family ($p=0.0230$, Figure 4C).

The presence of 'blebby' hemocytes was significantly higher in the digestive gland of spat exposed to OsHV-1 ($p=0.00671$, Figure 4B; Figure 5C-F) compared with controls. These hemocytes showed multiple protrusions which occasionally budded-off from the cytoplasm. Giemsa staining revealed these protrusions to be mostly basophilic in nature (Figure 5C); however, some were filled with acidic contents. For greater definition, further investigations with haematoxylin and eosin staining showed predominantly basophilic protrusions, some containing clear globules (Figure 5E-F).

3.3 Microbial analyses

A total of 15,920,350 16S rRNA reads (mean of 88,446 per sample) were sequenced, of which 78% remained after quality filtering, 70% after denoising and merging, and 66% after chimera removal (Supplementary Data 2). Removal of potential contamination, non-bacterial ASVs and rare ASVs further reduced read count by 25% for a total 7,935,417 sequence reads (mean of 66,684 reads per sample) and a total of 3,011 ASVs.

3.3.1. Composition of bacterial communities and alpha diversity in oysters.

We first analyzed the microbiota composition in tissue from recipient oysters over the course of the experimental infection. When examined as relative abundance in tissue, oysters carried three main bacterial phyla *Proteobacteria* (38%), *Bacteroidota* (27%), *Firmicutes* (21%), with small fractions (<20%) of *Myxococcota*, *Campilobacterota* and *Verrucomicrobiota*. The taxonomic profile at family and phylum levels were noticeably different between oyster and seawater microbiota, with no discernable difference based on Time and Infection (Figure 6).

Linear mixed-effects regression found no significant difference in alpha-diversity between families and infection status. However, a significant increase in alpha diversity was noticeable over time for resistant and highly resistant families (control and infected) for both richness and Shannon index (Additional Table A-B-C).

3.3.2 Composition of bacterial communities and alpha diversity in water.

Relative abundance of the bacterial phyla in the surrounding water showed that *Proteobacteria* were the dominant phylum (>70%) followed by *Bacteroidata* (>20%, Figure 6). Very low abundance of *Firmicutes* and *Campilobacterota* were detected in the water indicating a specificity to oyster tissue.

Using linear mixed-effects regression, no significant effect of 'infection' nor 'time' after start of experiment could be observed on the bacterial richness and Simpson index. Shannon index, however, did show a weak but significant negative effect (*p*-value = 0.05; R^2 = 0.06) of Infection (Additional Table A-B-C).

3.3.3 OsHV-1 infection induces deep change in beta diversity.

Beta-diversity (herein the extent of change in community composition) was assessed with a principal component analysis (PCA) to explore the potential influence of several factors including bacterial richness, family type (SR), viral replication (ORF), viral load and family. The PCA shows a clear clustering of host-microbiota based on treatment (infected vs controls) with evidence of effect of viral load and viral replication on oyster microbiota diversity and oyster survival rate (Figure 7).

Permutational analysis of variances confirmed that infection (p=0.001) and time (p=0.001) played a significant role in structuring microbial community composition in oysters with no effect of family type nor their interaction with infection (Table 2). Conversely, a significant difference in community composition could be observed between individual oyster families, but there was no significant interaction with these and infection (Sup Table 2).

Table 2: **Permutational analysis of variance of oyster microbial community composition with Infection, Family type, Time, and their interaction terms as factors**. Significant p-values are highlighted in bold.

Term	R^2	p-value
Infection	0.097	**0.001**
Family type	0.019	0.306
Time	0.037	**0.001**
Family type * Infection	0.017	0.371
Collection date * Family type	0.013	0.852
Residuals	0.461	

Significant p-values are highlighted in bold.

3.3.4 Core microbiome analysis

Analysis of the core microbiota indicated that overall, 14 bacterial genera were only carried by highly resistant oysters and 20 by vulnerable oysters (Sup figure 2 and Sup Table 3). Specifically, core analyses revealed that the microbiome of oysters was dominated by *Polaribacter* and *Aquimarina*, with marginal differences between vulnerable and highly resistant oyster families (Sup Figure 3A). Among these differences, *Acanthopleuribacter*, *Cohaesibacter*, *Marinifilum*, *Mycoplasma*, *Roseovarius*, *Vibrio* and *Vicingus* were more prevalent in highly resistant families while *Aquibacter*, *Amphritea*, *BD1-7, Flavirhabdus, Fusibacter*, *Salinirepens*, Woeseia and SVA0996 were more prevalent in vulnerable families (Sup Figure 3B).

3.3.5 Identification of bacteria associated with the disease, and their potential use to predict oyster mortality

Pearson correlations of the centered-log ratio abundance of bacterial genera showed a strong positive association of *Ketobacter*, *Algoriphagus*, *Maritimimonas*, *Marinomonas*, *Mycoplasma*, *Amphritea*, *Neptunibacter*, *Pontibacterium*, *Profundimonas*, Mf105b01, SM1A02 and *Psychrobium* with mortality rate and viral replication and/or viral load (Figure 8). Conversely, the presence of *Rubrivirga* and *Roseibacillus* was negatively correlated with mortality rate and/or viral load (Figure 8A). Network analysis showed significant positive interactions between several of these bacteria, including *Psychrobium* with *Profundimonas*, *Neptuniibacter* and *Algoriphagus*, and between *Mycoplasma*, *Neptuniibacter* and *Amphritea* (Figure 8B). The only significant and important (r>0.25) negative interactions were observed between *Roseibacillus* and Mf105b01, and SM1A02 and *Profundimonas*.

Figure 9 shows the relative abundance (A) and the prevalence (B) of bacterial genera correlated with mortality rate, viral replication, or viral load between vulnerable and highly resistant families in control or infected conditions. Interestingly, infection induced an increase in the relative abundance of *Mycoplasma*, *Amphritea* and *Psychrobium* whereas prevalence of *Mycoplasma, Amphritea, SM1A02* and *Neptuniibacter* was increased in infected oysters. Noticeably, the prevalence of *Ketobacter, Pontibacterium* and *Maritimimonas* strongly increased only in vulnerable families, as opposed to the prevalence of *Rubrivirga* which only increased in highly resistant families (Figure 9B). Figure 9 also shows that most of the taxa associated with POMS disease are present at low abundance in oyster before infection: *Mycoplasma, Amphritea, Ketobacter, Maritinomonas* or S1A02.

Figure 10 shows variables selected by random forest analysis to predict the outcome (positive or negative) of the POMS disease. Presence of *Mycoplasma* ASV-1 and *Ketobacter* in oyster tissues were the best predictor of the POMS outcome (> 60% relative importance), followed by ORF, *Cyclobacteriaceae, Pelagicoccus* and a second *Mycoplasma* ASV-2. To a lesser extent (< 5% relative importance), viral load in the surrounding water could also help predict mortality rate.

4. Discussion

In this study, we characterized the pathogenesis of POMS, the disease progression, and the associated changes in the microbiome of Pacific oysters from 10 contrasted families with variable genetically based resistance to POMS, following a lab-based infection with a purified isolate of OsHV-1. Our main findings are (1) a delay in viral infection resulting in a late onset of mortality compared with previous descriptions, and (2) an absence of major fatal bacteraemia in oysters during the POMS. Further, comparison of microbiota carried by the different vulnerable and resistant families allowed (3) the identification of potentially deleterious and beneficial bacterial taxa that can influence the outcome of the disease.

4.1. Temporal dynamics of POMS following OsHV-1 exposure in New Zealand

In vulnerable families, mortality started 48 h after oysters were exposed to 10^9 copies of OsHV-1 L^{-1}, whilst significant mortalities (> 10%) were recorded after 144 h to ultimately reach 50% at the end of the challenge (336 hpi). These results indicate a delayed viral infection in NZ compared to recent descriptions in Australia, the USA and France where the thresholds of 10% mortality were recorded at, respectively, 48 hpi [61, 62], 96 hpi [63], and 120 hpi [10, 16] using similar methods of infection and viral doses. In our study, delayed mortalities coincided with late expression of 3 common viral genes recorded after 96h. In France, high expression of the same viral genes (ORF27, 38 & 87) was detected in challenged oysters earlier, from 24 to 48 hpi [10, 16, 42]. However, in our experiment, viral load was maintained around 6.5 x 10^8 copies L^{-1} even after new filtered and UV treated seawater was reintroduced in the recipient tanks at 48 hpi, suggesting active viral replication and shedding of virions were occurring from 72 hpi.

Histological analyses performed after 72 hpi did not reveal any hemocytosis, diapedesis, inflammation or bacterial colonization in tissues as previously described in oysters infected with OsHV-1 [10, 64, 65]. Large, edematous areas resulting in the disorganization of the connective tissue in the mantle and digestive gland were observed however, indicating a deterioration of the general health of infected animals. Additionally, hemocyte ‘blebbing’ in the connective tissue of the digestive gland was observed more frequently in oysters exposed to OsHV-1. Such ‘blebbing’ may be endocytosis of OsHV-1 particles (macropinocytosis). Macropinocytosis and bleb formation have in the last few years emerged as a major mechanism for virus infection [66] and were observed in many viruses like the Kaposi’s sarcoma-associated herpesvirus [67] or the Canid herpesvirus [68]. The protrusions extending from hemocytes may also be indicative of viral release by budding through the nuclear envelope as has been observed in hemocytes of the gypsy moth infected with baculovirus [69]. Alternatively, the hemocyte ‘blebbing’ may be the early stages of apoptosis (zeiosis), during which the nucleus condenses, cytoplasm shrinks, and the cell membrane blebs [70, 71]. Apoptosis is a key mechanism of antiviral response inducing the abortion of viral multiplication and elimination of viral particles by premature lysis of infected cells [72, 73]. Although nuclear fragments were observed in hemocyte protrusions occasionally (Fig. 5D), the

majority did not contain obvious nuclear fragments (indicated by deep blue staining, Fig. 5C, E, F) and there was no notable increase in apoptosis or phagocytosis in this tissue.

4.2. Role of microbiota during POMS infection

In the present study, we found distinct taxonomic composition between oyster tissue and surrounding rearing seawater, a finding in agreement with other previous studies [30, 34, 74]. Despite maintaining oysters under common and controlled conditions (i.e., seawater UV treatment, constant temperature, optimal dissolved oxygen, hatchery-cultured algal feed), we also found significant changes in the composition of oyster microbiota throughout the experiment while bacterial composition and richness of the seawater were not affected by time, suggesting that oysters have a dynamic microbiome that can be selectively colonized by transient distinct bacterial taxa.

The oyster microbiota may also respond to or be modulated by stress experienced by the host, shifting towards an opportunist-dominated community that can affect the host's fitness and survivability. This is exemplified by OsHV-1 infection in the Pacific oyster which induces an immune suppression followed by the colonization of opportunistic bacteria in tissues, resulting in a dysbiosis that can lead to systemic infection and host death [10, 75]. This phenomenon is typically characterized by the proliferation of one or very few bacterial species leading to a drop in alpha-diversity, and increase in microbiota dispersion [10, 76].

Surprisingly, in the current study, bacterial profiling analyses did not show marked changes of alpha-diversity in oysters or water following OsHV-1 infection. However, significant changes in microbial beta-diversity were induced by infection regardless of oyster vulnerability phenotype. During infection, microbial community composition of oyster tissues was strongly correlated with viral load, viral replication, and survival rate as shown by PCoA / Bray Curtis statistical analyses. Furthermore, a limited number of bacterial families were significantly associated with mortality. Among these families, *Mycoplasma*, *Marinomonas*, *Psychrobium*, *Amphritea*, *Neptuniibacter* were the most abundant. These specific taxa have been previously described as opportunistic pathogenic bacteria contributing to systemic infection during POMS [19, 20, 22, 77], supporting the conservation of the POMS pathobiota across geographically distant environments and varied oyster genetics pedigrees [19, 77].

Importantly, two specific *Mycoplasma* strains were found to be among the most important bacteria in predicting mortality, following a OsHV-1 infection. *Mycoplasma* have the smallest known prokaryotic genome and consequently, are believed to be obligate commensals or parasites due to having limited metabolic capabilities [78]. They have been found in high proportions in various oyster species across a broad geographic range and have been considered as core microbes of the oyster's gut tissue [22, 79–81]. Nonetheless, some *Mycoplasma* strains are believed to become intracellular pathogens under environmental stress and to cause infections in bivalve mollusks [82–85]. Interestingly, *Mycoplasma* have apical bleb-like protrusion that helps them conglomerate or attach to host cells [83], potentially explaining the 'blebbing' in the connective tissue of the digestive gland observed in infected oysters.

Furthermore, we found that bacteria from the *Profundimonas* genus was highly correlated with intense viral replication; presence of this taxa was only evidenced in Australia, in the bacterial core of oyster presenting moderate mortalities following field-exposure to OsHV-1 [20]. Our study also characterized seven new bacterial genera in vulnerable oysters, all potentially implicated in the pathogenesis in New Zealand and not previously reported. Specifically, four members of the *Gammaproteobacteria* class, consisting of *Ketobacter*, *Pontibacterium*, *Profundimonas* and *Nitrosococcaceae*, and two members of the phylum Bacteroidetes (*Algoriphagus* and *Maritimimonas*) were identified. Network association analyses highlighted complex patterns of inter-relationships between these bacterial taxa and corresponding phenotypes like viral load, viral replication, and survival rates, suggesting a possible bacterial consortium associated with host colonization as previously described in France [77].

All together, these data reveal some variations in the course of the disease compared to previous descriptions carried out in other countries. Despite high viral concentration in the water, high mortality rates recorded in vulnerable families, and the presence of *Mycoplasma*, *Amphritea*, *Pontibacterium*, *Ketobacter* and *Maritimimonas* associated with infected individuals, oysters presented a delayed viral replication (based on ORF27, 38, and 87), and did not experience massive dysbiosis. In addition, amplicon sequencing did not reveal a notable abundance of taxa from the genus *Vibrio* associated with mortality. This finding differs from previous studies where naturally infected oysters commonly showed an increase in the load of *Vibrio* spp. as the disease progresses [7, 23, 25, 76]. The use of hatchery-born, OsHV-1-free oysters combined with purified isolate of OsHV-1 and filtered; UV sterilized seawater could explain the low prevalence of *Vibrio* spp. observed. Further research involving methodologies with higher taxonomic resolution (e.g., metagenomics) would be necessary to adequately identify the putative pathogenic strains detected in this study.

4.3. A distinct OsHV-1 variant specific to New Zealand

We can hypothesize that the delayed timing in the course of infection, the limited dysbiosis and the unusual features of hemocytes *via* histological observations may be the result of a distinct NZ OsHV-1 variant. During a mortality episode of Pacific oyster juveniles in the summer of 2010-11, Keeling et al. [7] analyzed the C2-C6 region of the OSHV-1 virus isolated in the North Island of NZ. The authors reported that the isolated sequence shared similar variations with the reference OsHV-1 *µ*Var. However, the NZ specimens were also carrying variations of two nucleotides common to the OsHV-1 reference strain (AY509253) diverging from *µ*Var [7]. Viruses generally exhibit high levels of genetic diversity, having the ability to produce diverse and genetically linked mutants. The level of *de novo* genetic diversity within viral populations likely influences viral pathogenicity, host determination, dissemination, and host immune evasion [86]. Prior to 2008 and the identification of OsHV-1 *µ*Var in France [4], two genotypes of OsHV-1 were identified: the reference strain [87] and a second genotype OsHV-1 Var detected in *Pecten maximus* [88]. With the recent advances in genomic sequencing efforts, considerable genotypic variations within the OsHV-1 species have been established. These variations are associated with different host species as well as temporal and geographical factors [89–91], supporting the possible emergence of specific variants in NZ.

4.4. Differences between vulnerable and resistant families

Another explanation for the different dynamics of viral infection and the absence of bacteraemia or apoptosis observed in oysters in the current study may be that what we term 'vulnerable' families could still have inherited some resistance traits from their parents. Indeed, the females used to produce our vulnerable families were a subset of oysters from families that showed poor survival but still survived at least two on-farm challenges to OsHV-1. Indeed, host immune ability to defend against OsHV-1 has been found to have a genetic basis in the Pacific oyster with resistance shown to be moderately to highly heritable [11, 12, 92]. Similarly, resistance against bacterial infection such as *Vibrio aestuarianus* has also been found to have a genetic component with moderate heritability [11], further highlighting the potential of selective breeding for increased disease resilience.

In this study, no significant difference in host-microbial taxonomic composition could be observed between family types (i.e., vulnerable, resistant, highly resistant). Nonetheless, *Neptuniibacter*, a bacterium strongly correlated with mortality rate and viral load, was solely found in vulnerable families, albeit in low abundance and prevalence. Interestingly, taxa highly associated with mortality rate and viral load such as *Ketobacter, Mycoplasma and Psychrobium* were similarly present in control specimens across family types (Fig. 8,C), indicating that their potential to cause a disease was reduced in highly resistant families. While no significant difference could be observed between family types, we did observe a significant effect of family (i.e., F1, F2, F4, etc.). This suggests a possible vertical transfer of bacteria and/or significant heritability of the microbiome composition in the Pacific oyster, which could affect OsHV-1 infection outcome. Such effect, including resistance to strains with potential pathogenicity, represent attractive future avenues of research to limit the severity of OsHV-1 outbreaks.

Moreover, among the ten oyster families exposed to OsHV-1 under common and controlled conditions, we obtained a range of mortality dynamics, survivorship (ranging from 99.3–50.8%) and viral replication (magnitudes of ORF expression from 0 to 10 000 in relative expression). For example, Family 1, exhibited a OsHV-1 resistance (i.e., ability to control pathogen burden, 99.3% survival and very low viral replication) while Family 2 and 3 seems resilient to the infection (i.e., ability to maintain performance while infected, medium viral replication and survival > 82%). This illustrates the complexity of POMS in the Pacific oyster and, together with eventual specific variation of OsHV-1, may explain the diversity of host x pathogen interactions observed in different producing countries worldwide. Molecular analyses (transcriptome sequencing) of the mechanisms underlying the contrasted responses to the disease and genome-wide association studies (GWAS) would greatly contribute to the identification of valuable candidate genes for selective breeding and improve productivity in the presence of POMS.

5. Conclusions

Characterization of bacterial communities associated with oyster spat infected with POMS in a controlled environment can assist in understanding the role and function of the microbiome in disease resistance in *C. gigas*. The development of selective breeding in aquaculture [93] will also provide increasing

opportunities to access material showing contrasted phenotypes, allowing for a better understanding of the molecular bases of complex traits, such as resistance to POMS in *C. gigas*. Collectively, these results could improve current disease management and aquaculture practices. Furthermore, the use of 16S rRNA gene sequencing/metabarcoding and the identification of bacterial species as a predictive factor to determine survival of oysters may open new perspectives as a phenotyping tool during selective breeding and/or a diagnostic tool to determine shellfish health.

As with any microbiome study, there are limitations in amplicon sequencing and deriving conclusions on relative (non-absolute) bacterial proportion and quantification should be done cautiously. Future studies should include targeted quantification of specific bacteria or attempt to normalize ASV abundance with qPCR of the total bacterial community [21, 22]. Metagenomic association-wide study could also help us identify the key genes from specific strains that may be negatively affecting oysters' health, revealing essential clues on their role in pathogenicity and adaptability.

Declarations

Ethics approval and consent to participate: The study was conducted according to the guidelines of the Declaration of Helsinki and approval of the Animal Ethics Committee was not applicable for the use of oysters.

Availability of data and material: The dataset(s) supporting the conclusions of this article are available in the NCBI repository [PRJNA832870].

Competing interests: The authors declare no competing or financial interests.

Funding: was provided by the NZ Government's Ministry of Business, Innovation and Employment through the Cawthron Shellfish Aquaculture programme [contract no. CAWX1801] and the Royal Society of NZ through the Catalyst Leaders: International Leader Fellowship Fund [contract no. ILF-CAW-1801].

Authors' contributions: LD, JV, PB and ZH conception and design. LD, JV, JF B, JB, PB, AR and JV, ZH data collection and performance lab trials, LD, JB, XP preparation of samples for sequencing. AR histopathological assessments, OL bioinformatic analyses. LD, JV, AR, OL writing. All authors: revision/editing. Funding: JV and ZH. All authors read and approved the final manuscript.

Acknowledgements: We are extremely grateful to Jim Dollimore and Will McKay at Biomarine Ltd for provision of adult broodstock, and to Hannah Mae and the rest of the hatchery team at the Cawthron Aquaculture Park for the technical support to produce the biological material. We also thank Karthiga Kumanan, Bridget Finnie, Shenae Muirhead and Joanna Copedo for their invaluable help during the challenge and sampling. Thank you to the molecular team (Branwen Trochel, Ulla von Ammon) for technical assistance, and to Isabelle Arzul and Steve Webb for histological advice.

References

1. Barbosa-Solomieu V, Dégremont L, Vázquez-Juárez R, Ascencio-Valle F, Boudry P, Renault T. Ostreid Herpesvirus 1 (OsHV-1) detection among three successive generations of Pacific oysters (*Crassostrea gigas*). Virus Res. 2005;107:47–56.
2. EFSA. Scientific opinion on the increased mortality events in Pacific oysters. Eur Food Saf Auth J. 2010;8:1–60.
3. Pernet F, Lupo C, Bacher C, Whittington RJ. Infectious diseases in oyster aquaculture require a new integrated approach. Philos Trans R Soc B Biol Sci. 2016;371.
4. Segarra A, Pépin JF, Arzul I, Morga B, Faury N, Renault T. Detection and description of a particular Ostreid herpesvirus 1 genotype associated with massive mortality outbreaks of Pacific oysters, *Crassostrea gigas*, in France in 2008. Virus Res. 2010;153:92–9.
5. EFSA. Oyster mortality. EFSA J. 2015;13:4122. Available from: http://doi.wiley.com/10.2903/j.efsa.2015.4122
6. Jenkins C, Hick P, Gabor M, Spiers Z, Fell S, Gu X, et al. Identification and characterization of an Ostreid herpesvirus-1 microvariant (OsHV-1 µ-var) in *Crassostrea gigas* (Pacific oysters) in Australia. Dis Aquat Organ. 2013;105:109–26.
7. Keeling SE, Brosnahan CL, Williams R, Gias E, Hannah M, Bueno R, et al. New Zealand juvenile oyster mortality associated with ostreid herpesvirus 1-an opportunistic longitudinal study. Dis Aquat Organ. 2014;109:231–9.
8. Hwang JY, Park JJ, Yu HJ, Hur YB, Arzul I, Couraleau Y, et al. Ostreid herpesvirus 1 infection in farmed Pacific oyster larvae *Crassostrea gigas* (Thunberg) in Korea. J Fish Dis. 2013;36:969–72.
9. Burge CA, Friedman CS, Kachmar ML, Humphrey KL, Moore JD, Elston RA. The first detection of a novel OsHV-1 microvariant in San Diego, California, USA. J Invertebr Pathol. 2021;184:107636.
10. De Lorgeril J, Lucasson A, Petton B, Toulza E, Montagnani C, Clerissi C, et al. Immune-suppression by OsHV-1 viral infection causes fatal bacteraemia in Pacific oysters. Nat Commun. 2018;9:4215.
11. Azéma P, Lamy JB, Boudry P, Renault T, Travers MA, Dégremont L. Genetic parameters of resistance to *Vibrio aestuarianus*, and OsHV - 1 infections in the Pacific oyster, *Crassostrea gigas*, at three different life stages. Genet Sel Evol. BioMed Central; 2017;1–16.
12. Camara MD, Yen S, Kaspar HF, Kesarcodi-Watson A, King N, Jeffs AG, et al. Assessment of heat shock and laboratory virus challenges to selectively breed for Ostreid Herpesvirus 1 (OsHV-1) resistance in the Pacific oyster, *Crassostrea gigas*. Aquaculture. Elsevier B.V.; 2017;469:50–8.
13. Hick PM, Evans O, Rubio A, Dhand NK, Whittington RJ. Both age and size influence susceptibility of Pacific oysters (*Crassostrea gigas*) to disease caused by Ostreid herpesvirus-1 (OsHV-1) in replicated field and laboratory experiments. Aquaculture.
14. Lorgeril J De, Petton B, Lucasson A, Perez V, Stenger P, Dégremont L, et al. Differential basal expression of immune genes confers *Crassostrea gigas* resistance to Pacific oyster mortality syndrome. BMC Genomics; 2020;1–15.
15. Pernet F, Tamayo D, Fuhrmann M, Petton B. Deciphering the effect of food availability, growth and host condition on disease susceptibility in a marine invertebrate. J Exp Biol. 2019;222:jeb210534.

16. Delisle L, Petton B, Burguin J-F, Morga B, Corporeau C, Pernet F. Temperature modulates disease susceptibility of the Pacific oyster *Crassostrea gigas* and virulence of the Ostreid herpesvirus type 1. Fish Shellfish Immunol. Elsevier; 2018;80:71–9.
17. Pernet F, Tamayo D, Petton B. Influence of low temperatures on the survival of the Pacific oyster (*Crassostrea gigas*) infected with ostreid herpes virus type 1. Aquaculture. Elsevier B.V.; 2015;445:57–62.
18. Petton B, Pernet F, Robert R, Boudry P. Temperature influence on pathogen transmission and subsequent mortalities in juvenile pacific oysters *Crassostrea gigas*. Aquac Environ Interact. 2013;3:257–73.
19. Clerissi C, de Lorgeril J, Petton B, Lucasson A, Escoubas JM, Gueguen Y, et al. Microbiota Composition and Evenness Predict Survival Rate of Oysters Confronted to Pacific Oyster Mortality Syndrome. Front Microbiol. 2020;11:1–11.
20. King WL, Jenkins C, Go J, Siboni N, Seymour JR, Labbate M. Characterisation of the Pacific Oyster Microbiome During a Summer Mortality Event. Microb Ecol. Microbial Ecology; 2019;77:502–12.
21. King WL, Kaestli M, Siboni N, Padovan A, Christian K, Mills D, et al. Pearl Oyster bacterial community structure is governed by location and tissue-type, but *Vibrio* species are shared among oyster tissues. Front Microbiol. Frontiers Media S.A.; 2021;12:723649.
22. Lasa A, di Cesare A, Tassistro G, Borello A, Gualdi S, Furones D, et al. Dynamics of the Pacific oyster pathobiota during mortality episodes in Europe assessed by 16S rRNA gene profiling and a new target enrichment next-generation sequencing strategy. Environ Microbiol. 2019;21:4548–62.
23. Pathirana E, Fuhrmann M, Whittington R, Hick P. Influence of environment on the pathogenesis of Ostreid herpesvirus-1 (OsHV-1) infections in Pacific oysters (*Crassostrea gigas*) through differential microbiome responses. Heliyon. Elsevier Ltd; 2019;5:e02101.
24. Lemire A, Goudenège D, Versigny T, Petton B, Calteau A, Labreuche Y, et al. Populations, not clones, are the unit of vibrio pathogenesis in naturally infected oysters. ISME J. 2015;9:1523–31.
25. Petton B, Bruto M, James A, Labreuche Y, Alunno-Bruscia M, Le Roux F. *Crassostrea gigas* mortality in France: The usual suspect, a herpes virus, may not be the killer in this polymicrobial opportunistic disease. Front Microbiol. 2015;6:1–10.
26. King WL, Siboni N, Williams NLR, Kahlke T, Nguyen KV, Jenkins C, et al. Variability in the Composition of Pacific Oyster Microbiomes Across Oyster Families Exhibiting Different Levels of Susceptibility to OsHV-1 µ var Disease. 2019;10:1–12.
27. Kamada N, Chen GY, Inohara N, Núñez G. Control of pathogens and pathobionts by the gut microbiota. Nat Immunol. 2013;14:685–90.
28. Defer D, Desriac F, Henry J, Bourgougnon N, Baudy-Floc'h M, Brillet B, et al. Antimicrobial peptides in oyster hemolymph: The bacterial connection. Fish Shellfish Immunol. Elsevier Ltd; 2013;34:1439–47.
29. Desriac F, Harras A El, Simon M, Bondon A, Brillet B, Chevalier P Le, et al. Alterins produced by oyster-associated *Pseudoalteromonas* are antibacterial cyclolipopeptides with LPS-Binding activity. Mar Drugs. 2020;18:630.

30. Stevick RJ, Sohn S, Modak TH, Nelson DR, Rowley DC, Tammi K, et al. Bacterial community dynamics in an oyster hatchery in response to probiotic treatment. Front Microbiol. 2019;10:1–13.
31. Wenjing Z, Tao Y, Christine P, J. SE, W. SC, C. RD, et al. The Probiotic bacterium *Phaeobacter inhibens* downregulates Virulence Factor Transcription in the shellfish pathogen *Vibrio coralliilyticus* by N-Acyl Homoserine Lactone production. Appl Environ Microbiol. American Society for Microbiology; 2021;85:e01545-18.
32. Hine P., Wesney B, Hay B. Herpesviruses associated with mortalities among hatchery-reared larval Pacific oysters *Crassostrea gigas*. Dis Aquat Org. 1992;135–42.
33. Adams SL, Smith JF, Roberts RD, Janke AR, Kaspar HF, Robin Tervit H, et al. Cryopreservation of sperm of the Pacific oyster (*Crassostrea gigas*): development of a practical method for commercial spat production. Aquaculture. 2004;242:271–82.
34. Vignier J, Laroche O, Rolton A, Wadsworth P, Kumanan K, Trochel B, et al. Dietary Exposure of Pacific Oyster (*Crassostrea gigas*) Larvae to Compromised Microalgae Results in Impaired Fitness and Microbiome Shift. Front Microbiol. 2021;12:0–19.
35. Ragg NLC, King N, Watts E, Morrish J. Optimising the delivery of the key dietary diatom *Chaetoceros calcitrans* to intensively cultured Greenshell™ mussel larvae, *Perna canaliculus*. Aquaculture. Elsevier B.V.; 2010;306:270–80.
36. Martenot C, Oden E, Travaillé E, Malas JP, Houssin M. Comparison of two real-time PCR methods for detection of ostreid herpesvirus 1 in the Pacific oyster Crassostrea gigas. J Virol methods. Elsevier B.V.; 2010;170:86–9.
37. Pernet F, Lugué K, Petton B. Competition for food reduces disease susceptibility in a marine invertebrate. Ecosphere. 2021;12.
38. Suquet M, De Kermoysan G, Araya RG, Queau I, Lebrun L, Le Souchu P, et al. Anesthesia in Pacific oyster, *Crassostrea gigas*. Aquat Living Resour . 2009;22:29–34.
39. Herlemann DPR, Labrenz M, Jürgens K, Bertilsson S, Waniek JJ, Andersson AF. Transitions in bacterial communities along the 2000 km salinity gradient of the Baltic Sea. ISME J. 2011;5:1571–9.
40. Klindworth A, Pruesse E, Schweer T, Peplies J, Quast C, Horn M, et al. Evaluation of general 16S ribosomal RNA gene PCR primers for classical and next-generation sequencing-based diversity studies. Nucleic Acids Res. 2013;41:1–11.
41. Kozich JJ, Westcott SL, Baxter NT, Highlander SK, Schloss PD. Development of a dual-index sequencing strategy and curation pipeline for analyzing amplicon sequence data on the miseq illumina sequencing platform. Appl Environ Microbiol. 2013;79:5112–20.
42. Segarra A, Faury N, Pépin JF, Renault T. Transcriptomic study of 39 ostreid herpesvirus 1 genes during an experimental infection. J Invertebr Pathol. 2014;119:5–11.
43. Martin M. Cutadapt removes adapter sequence from high-throughput sequencing reads. EMBnetJournal. 2011;17(1).
44. Callahan BJ, Mcmurdie PJ, Rosen MJ, Han AW, A AJ. DADA2: High resolution sample inference from Illumina amplicon data. 2016;13:581–3.

45. Wang Q, Garrity GM, Tiedje JM, Cole JR, Al WET. Naıve Bayesian Classifier for Rapid Assignment of rRNA Sequences into the New Bacterial Taxonomy. Appl Environ Microbiol. 2007;73:5261–7.
46. Quast C, Pruesse E, Yilmaz P, Gerken J, Schweer T, Glo FO, et al. The SILVA ribosomal RNA gene database project : improved data processing and web-based tools. Nucleic Acids Res. 2013;41:590–6.
47. McKnight DT, Huerlimann R, Bower DS, Schwarzkopf L, Alford RA, Zenger KR. microDecon: A highly accurate read-subtraction tool for the post-sequencing removal of contamination in metabarcoding studies. Environ DNA. John Wiley & Sons, Ltd; 2019;1:14–25.
48. Oksanen J, Blanchet FG, Friendly M, Kindt R, Legendre P, McGlinn D, et al. Vegan: Community Ecology Package. 2020. Available from: https://cran.r-project.org/package=vegan
49. Therneau T, Grambsch PM. Modeling Survival Data: Extending the Cox Model. Statistics. New York: Springer; 2000.
50. Cox DR. Regression Models and Life-Tables. J R Stat Soc Ser B. 1972;34:187–202.
51. Schoenfeld D. Partial residuals for the proportional hazards regression model. Biometrika. 1982;69:239–41.
52. Saeed AI, Sharov V, White J, Li J, Liang W, Bhagabati N, et al. TM4: A free, open-source system for microarray data management and analysis. Biotechniques. 2003;34:374–8.
53. Hadley Wickham. ggplot2: Elegant Graphics for Data Analysis. New York: Springer-Verlag New York; 2016. Available from: http://ggplot2.org
54. Mcmurdie PJ, Holmes S. phyloseq : An R Package for Reproducible Interactive Analysis and Graphics of Microbiome Census Data. PLoS One. 2013;8.
55. Bates D, Mächler M, Bolker BM, Walker SC. Fitting Linear Mixed-Effects Models Using lme4. J Stat Softw. 2015;67.
56. Lahti L, Shetty S. microbiome R package. 2019. Available from: http://microbiome.github.io
57. Gu Z, Eils R, Schlesner M. Complex heatmaps reveal patterns and correlations in multidimensional genomic data. Bioinformatics. 2016;32:2847–9.
58. Kassambara A. ggcorrplot: Visualization of a Correlation Matrix using “ggplot2”. 2019. Available from: https://cran.r-project.org/package=ggcorrplot
59. Faust K, Raes J. CoNet app: Inference of biological association networks using Cytoscape. F1000Research. 2016;5:1–14.
60. Kuhn M. caret: Classification and Regression Training. 2020. Available from: https://cran.r-project.org/package=caret
61. Burge CA, Reece KS, Dhar AK, Kirkland P, Morga B, Dégremont L, et al. First comparison of French and Australian OsHV-1 µvars by bath exposure. Dis Aquat Organ. 2020;138:137–44.
62. Cain G, Liu O, Whittington RJ, Hick PM. Reduction in virulence over time in ostreid herpesvirus 1 (Oshv-1) microvariants between 2011 and 2015 in Australia. Viruses. 2021;13.

63. Agnew MV, Friedman CS, Langdon C, Divilov K, Schoolfield B, Morga B, et al. Differential mortality and high viral load in naive pacific oyster families exposed to oshv-1 suggests tolerance rather than resistance to infection. Pathogens. 2020;9:1–18.
64. Friedman CS, Cherr GN, Clegg JS, Hamdoun, A. H., Jacobsen JL, Jackson, S. A., & Uhlinger KR. Investigation of the stress response, summer mortality and disease resistance of oysters, *Crassostrea gigas* and *Crassostrea virginica*. J Shellfish Res. 1999;18:297.
65. Renault T, Cochennec N, Le Deuff R-M, Chollet B. Herpes-like virus infecting Japanese oyster (*Crassostrea gigas*) spat. Bull Eur Assoc Fish Pathol. 1994;14:64–6.
66. Mercer J, Helenius A. Gulping rather than sipping: Macropinocytosis as a way of virus entry. Curr Opin Microbiol. Elsevier Ltd; 2012;15:490–9.
67. Sayan C, Mohanan V, Sathish S, Nitika P, Bala C. c-Cbl-Mediated Selective Virus-Receptor Translocations into Lipid Rafts Regulate Productive Kaposi's Sarcoma-Associated Herpesvirus Infection in Endothelial Cells. J Virol . American Society for Microbiology; 2011;85:12410–30.
68. Eisa M, Loucif H, van Grevenynghe J, Pearson A. Entry of the Varicellovirus Canid herpesvirus 1 into Madin–Darby canine kidney epithelial cells is pH-independent and occurs via a macropinocytosis-like mechanism but without increase in fluid uptake. Cell Microbiol. 2021;23:1–18.
69. Nappi AJ, Hammill TM. Viral release and membrane acquisition by budding through the nuclear envelope of hemocytes of the gypsy moth, *Porthetria dispar*. J Invertebr Pathol. 1975;26:387–92
70. Cohen JJ, Duke RC, Fadok VA, Sellins KS. Apoptosis and Programmed Cell Death in Immunity. Annu Rev Immunol. Annual Reviews; 1992;10:267–93.
71. White E. Life, death, and the pursuit of apoptosis. Genes Dev. 1996;10:1–15.
72. Pilder S, Logan J, Shenk T. Deletion of the Gene Encoding the Adenovirus 5 Early Region. 1984;52:664–71.
73. Segarra A, Mauduit F, Faury N, Trancart S, Dégremont L, Tourbiez D, et al. Dual transcriptomics of virus-host interactions: comparing two Pacific oyster families presenting contrasted susceptibility to ostreid herpesvirus 1. BMC Genomics. 2014;15:580.
74. Arfken A, Song B, Allen SK, Carnegie RB. Comparing larval microbiomes of the eastern oyster (*Crassostrea virginica*) raised in different hatcheries. Aquaculture. 2021;531:735955.
75. Petton B, Destoumieux-garzo D, Pernet F, Toulza E, De Lorgeril J, Degremont L, et al. The Pacific Oyster Mortality Syndrome , a Polymicrobial and Multifactorial Disease : State of Knowledge and Future Directions. 2021;12:1–10.
76. Lokmer A, Wegner KM. Hemolymph microbiome of Pacific oysters in response to temperature, temperature stress and infection. Nature Publishing Group; 2015;670–82.
77. Lucasson A, Luo X, Shogofa M, De Lorgeril J, Toulza E, Petton B, et al. A core of functionally complementary bacteria colonizes oysters in Pacific Oyster Mortality Syndrome. 2020;
78. Aceves AK, Johnson P, Bullard SA, Lafrentz S, Arias CR. Description and characterization of the digestive gland microbiome in the freshwater mussel *Villosa nebulosa(Bivalvia: Unionidae*). J

Molluscan Stud. 2018;84:240–6.

79. King GM, Judd C, Kuske CR, Smith C. Analysis of Stomach and Gut Microbiomes of the Eastern Oyster (*Crassostrea virginica*) from Coastal Louisiana, USA. PLoS One. 2012;7.
80. Offret C, Paulino S, Gauthier O, Chateau K, Bidault A, Corporeau C, et al. The marine intertidal zone shapes oyster and clam digestive bacterial microbiota. FEMS Microbiol Ecol. 2020;96.
81. Pierce ML, Ward EJ. Gut Microbiomes of the Eastern Oyster (*Crassostrea virginica*) and the Blue Mussel (*Mytilus edulis*): Temporal Variation and the Influence of Marine Aggregate-Associated Microbial Communities. 2019;4:1–17.
82. Azevedo C. Occurrence of an unusual branchial mycoplasma-like infection in cockle *Cerastoderma edule* (*Molusca, Bivalvia*). Dis Aquat Organ. 1993;16:55–9.
83. Hine PM, Diggles BK. Prokaryote infections in the New Zealand scallops *Pecten novaezelandiae* and *Chlamys delicatula*. Dis Aquat Organ. 2002;50:137–44.
84. Brown DR, Zacher LA, Wendland LD, Brown MB. Emerging mycoplasmoses in wildlife. Blanchard A, Browning Glenn, editors. Mycoplasmas Mol Biol Strateg Control. Horizon bi. 2005. p. 383–414.
85. Paillard C, Le Roux F, Borrego JJ. Bacterial disease in marine bivalves, a review of recent studies: Trends and evolution. Aquat Living Resour. 2004/12/15. EDP Sciences; 2004;17:477–98.
86. Sanjuán R, Domingo-Calap P. Mechanisms of viral mutation. Cell Mol Life Sci. 2016;73:4433–48.
87. Davison AJ, Trus BL, Cheng N, Steven A, Watson MS, Cunningham C, et al. A novel class of herpesvirus with bivalve hosts. J Gen Virol. 2005;86:41–53.
88. Arzul I, Nicolas J-L, Davison AJ, Renault T. French Scallops: A New Host for Ostreid Herpesvirus-1. Virology . 2001;290:342–9.
89. Bai CM, Morga B, Rosani U, Shi J, Li C, Xin LS, et al. Long-range PCR and high-throughput sequencing of Ostreid herpesvirus 1 indicate high genetic diversity and complex evolution process. Virology. Elsevier Inc.; 2019;526:81–90.
90. Delmotte J, Chaparro C, Galinier R, Lorgeril J De, Petton B, Stenger P, et al. Contribution of Viral Genomic Diversity to Oyster Susceptibility in the Pacific Oyster Mortality Syndrome. 2020;11:1–17.
91. Morga B, Jacquot M, Pelletier C, Chevignon G, Dégremont L, Biétry A, et al. Genomic Diversity of the Ostreid Herpesvirus Type 1 Across Time and Location and Among Host Species. 2021;12:1–13.
92. Divilov K, Schoolfield B, Morga B, Dégremont L, Burge CA, Mancilla Cortez D, et al. First evaluation of resistance to both a California OsHV-1 variant and a French OsHV-1 microvariant in Pacific oysters. BMC Genet. BMC Genetics; 2019;20:96.
93. Boudry P, Allal F, Aslam ML, Bargelloni L, Bean TP, Brard-Fudulea S, et al. Current status and potential of genomic selection to improve selective breeding in the main aquaculture species of International Council for the Exploration of the Sea (ICES) member countries. Aquac Reports. 2021;20.

Figures

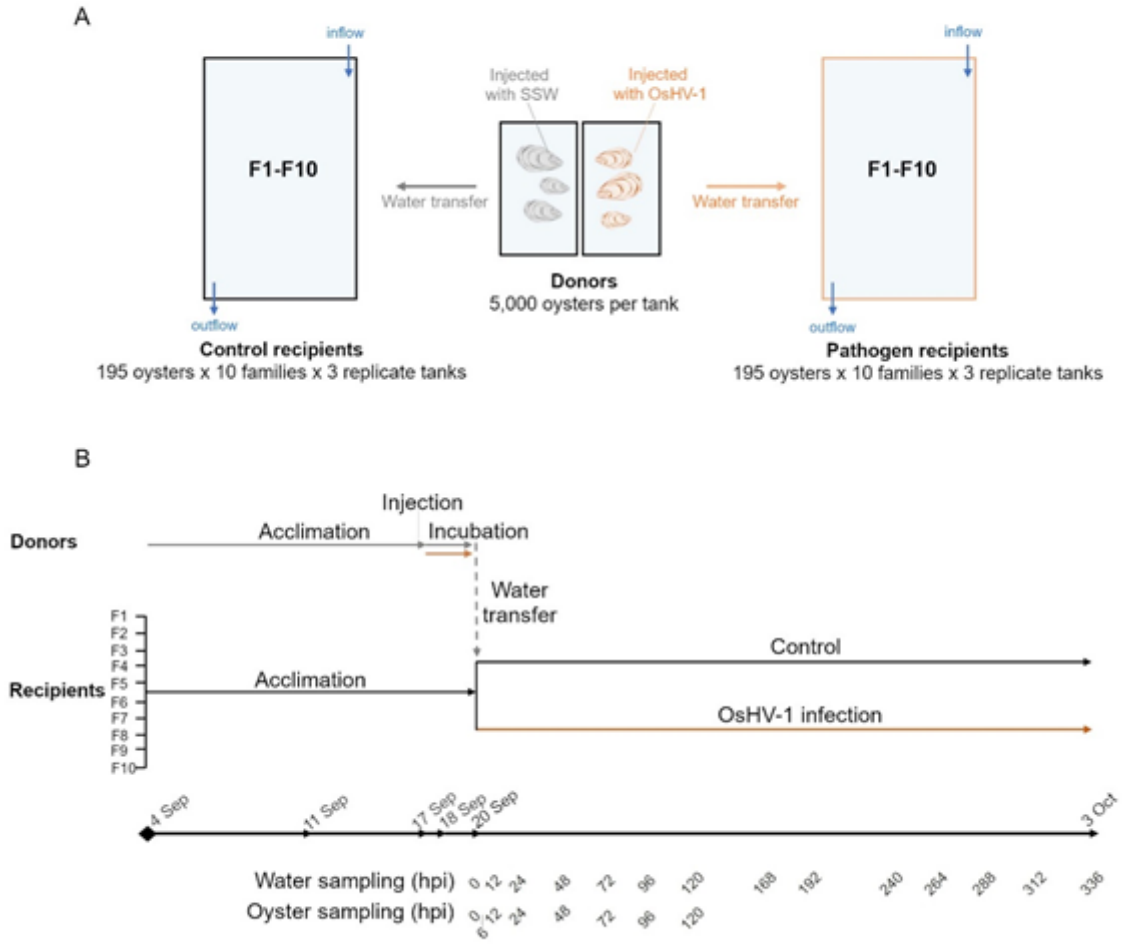

Figure 1

Experimental design to investigate the disease progression and the susceptibility of ten oyster families exposed to the Ostreid herpesvirus type 1. (A) Donors and recipient oysters, (B) Experimental timeline. OsHV-1: Ostreid herpes virus type 1, SSW: Sterile artificial sea water, hpi: hour post-infection.

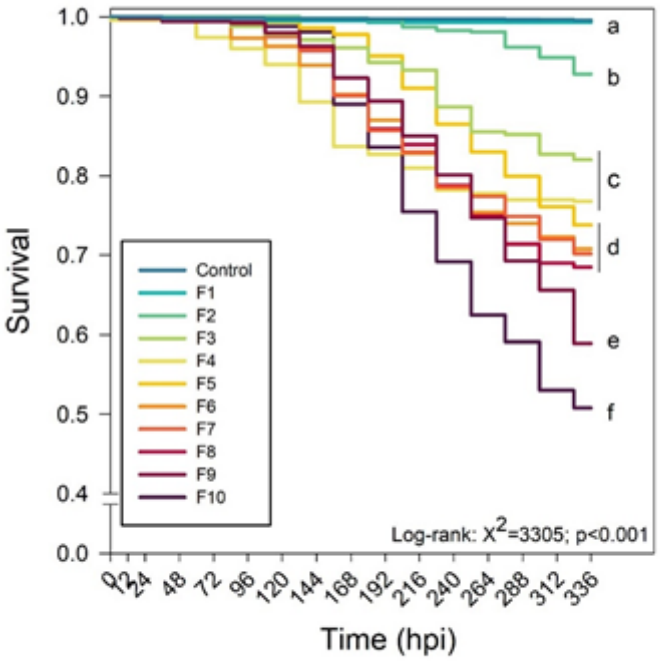

Figure 2

Survival of oyster (OsHV-1 exposed recipient oysters) in each family (F1 – F10) challenged with OsHV-1. "Control" group represents a mean survival of all recipient oysters challenged with SSW. Values are means (n = 3 replicate tanks) and letters indicate significant differences, Log-rank: Chi square=3305, p-value< 0.001. hpi: hours post-infection.

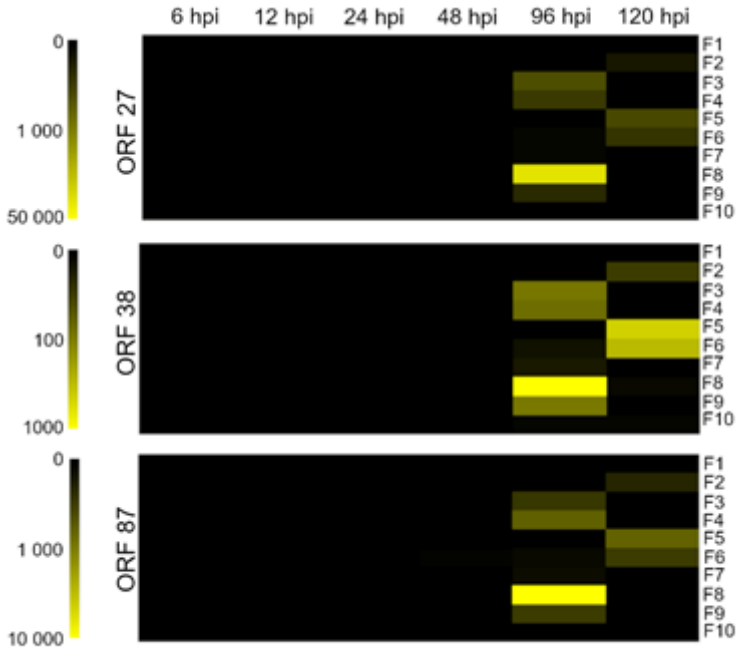

Figure 3

Heatmap presenting the relative expression of three OSHV-1 open reading frames - ORF 27, 38 and 87 - expressed in oysters from ten different families (F1-F10) as a function of time in hours post infection (hpi). Colour intensity indicates the magnitude of ORF expression in copies per mg of oyster.

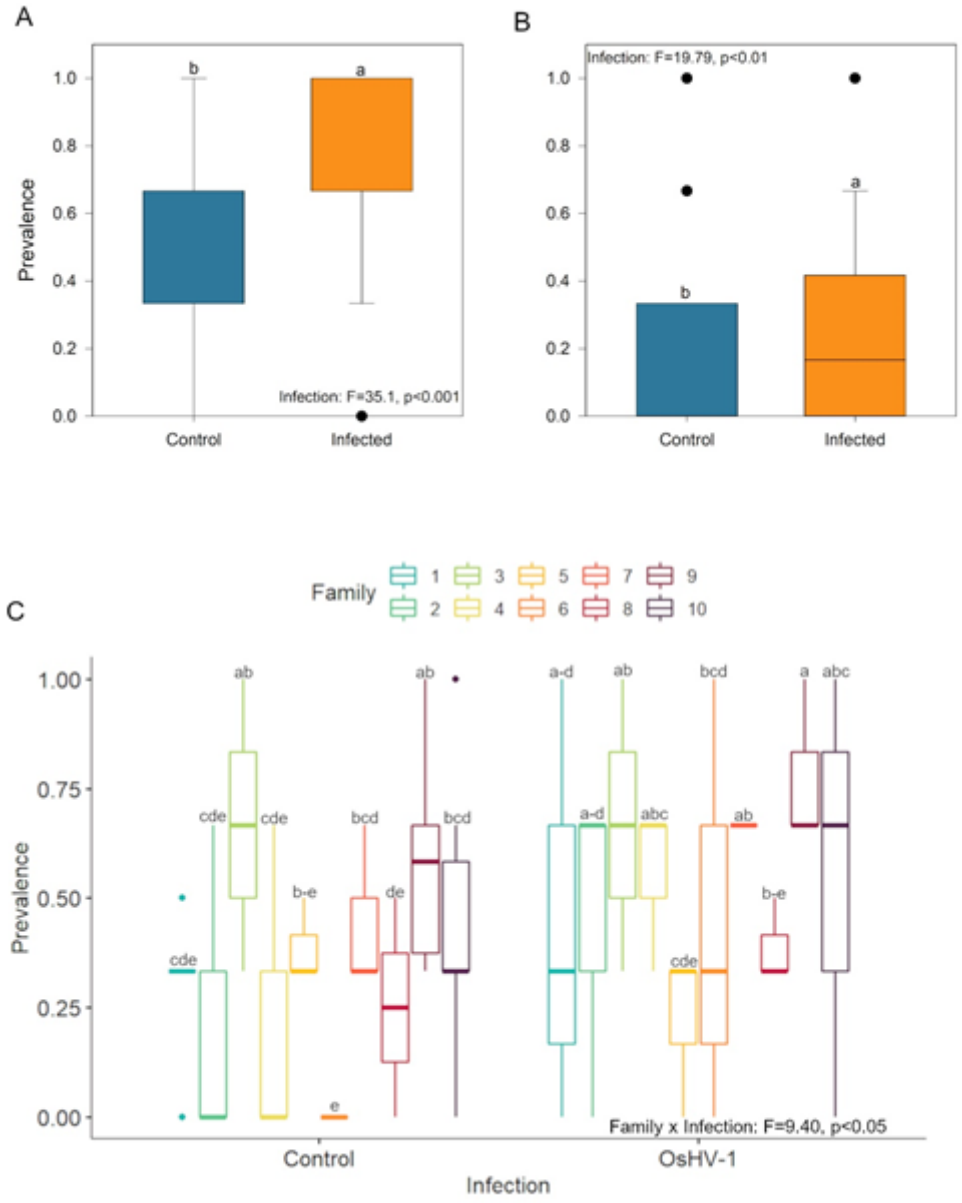

Figure 4

Histological assessments. The prevalence of A) 'loose' connective tissue and B) 'blebby' hemocytes in the digestive gland of control and OsHV1-infected oysters at 0 and 72 hpi (all families combined). C) The prevalence of loose connective tissue in the mantle of oysters from all families (F1 to F10) assessed at 0 and 72 hpi, in the control and OsHV1-exposed oysters. Treatments with the same letter were not significantly different (p> 0.05).

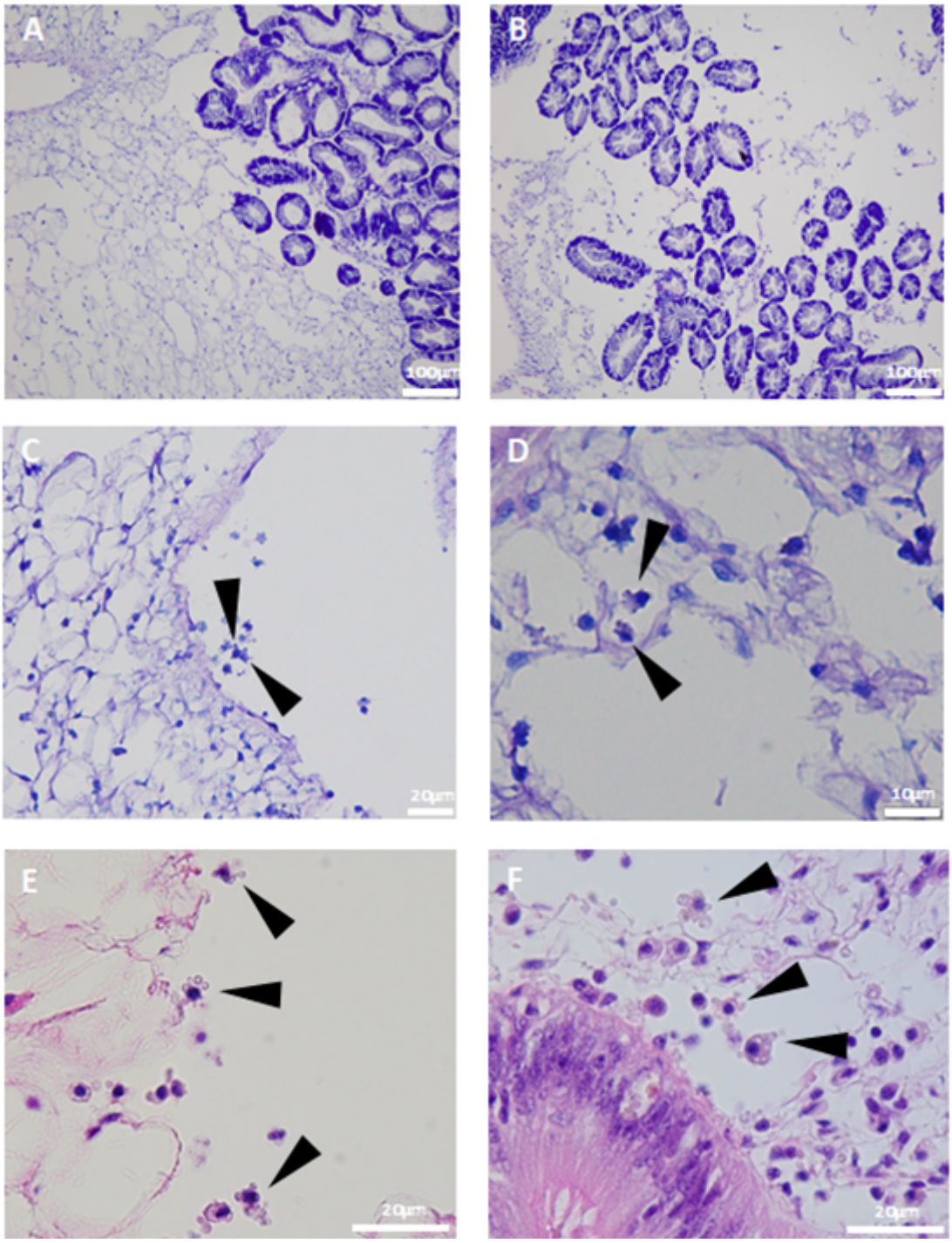

Figure 5

Examples of histopathological features observed in *Crassostrea gigas* spat infected with OsHV-1. An example of normal (A) and 'loose' (B) connective tissue in the digestive gland, showing a loss of structure and large edematous areas around the digestive tubules. Examples of 'blebby' hemocytes (black arrows) in a blood space in the digestive gland (C and E), and in the connective tissue around the digestive gland (D and F). Tissues in micrographs C and D are stained with Giemsa and those in E and F are stained with haematoxylin and eosin.

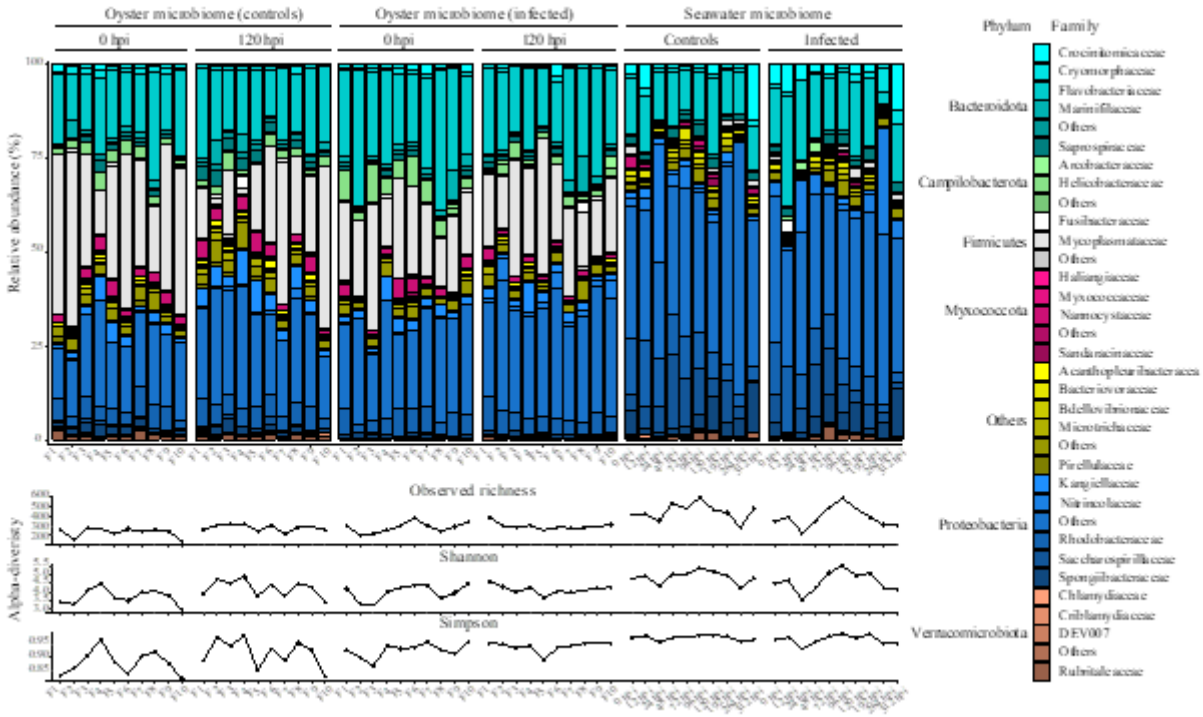

Figure 6

Relative abundance of the most important bacterial families and phyla (upper panels) and alpha-diversity (richness, Shannon, Simpson; bottom figure) values per sample type (oyster microbiota vs seawater), treatment (control vs infected) and time. Bacterial families that were not among the first 5 most abundant families within each phylum were grouped under 'Others'. Similarly, phyla that were not among the first 6 most abundant phyla were grouped under "Others".

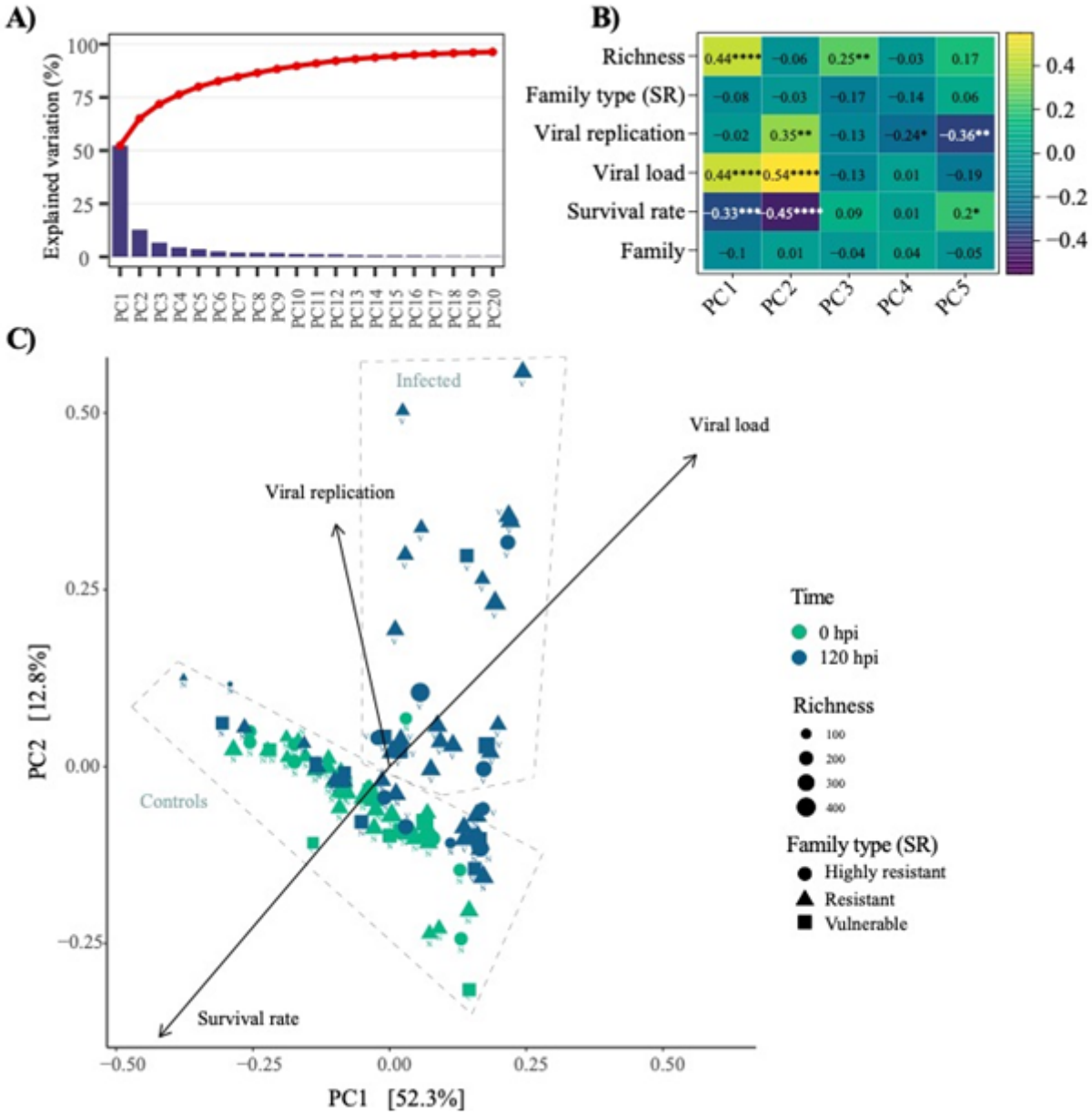

Figure 7

Beta-diversity analysis of host microbiome using a principal component analysis. A) Percent of variance explained per Principal Component (PC). B) Pearson correlation of variables of interest with each component with level of significance (p-value) indicated by the number of asterisk (* p= 0.05; ** p=0.01; *** p=0.001 **** p=0.0001). C) Principal component analysis including overlaid variables such as viral load, viral replication and survival rate associated with the first two components. N: non-infected oyster samples (control); V: virus-infected oyster samples (recipient oysters).

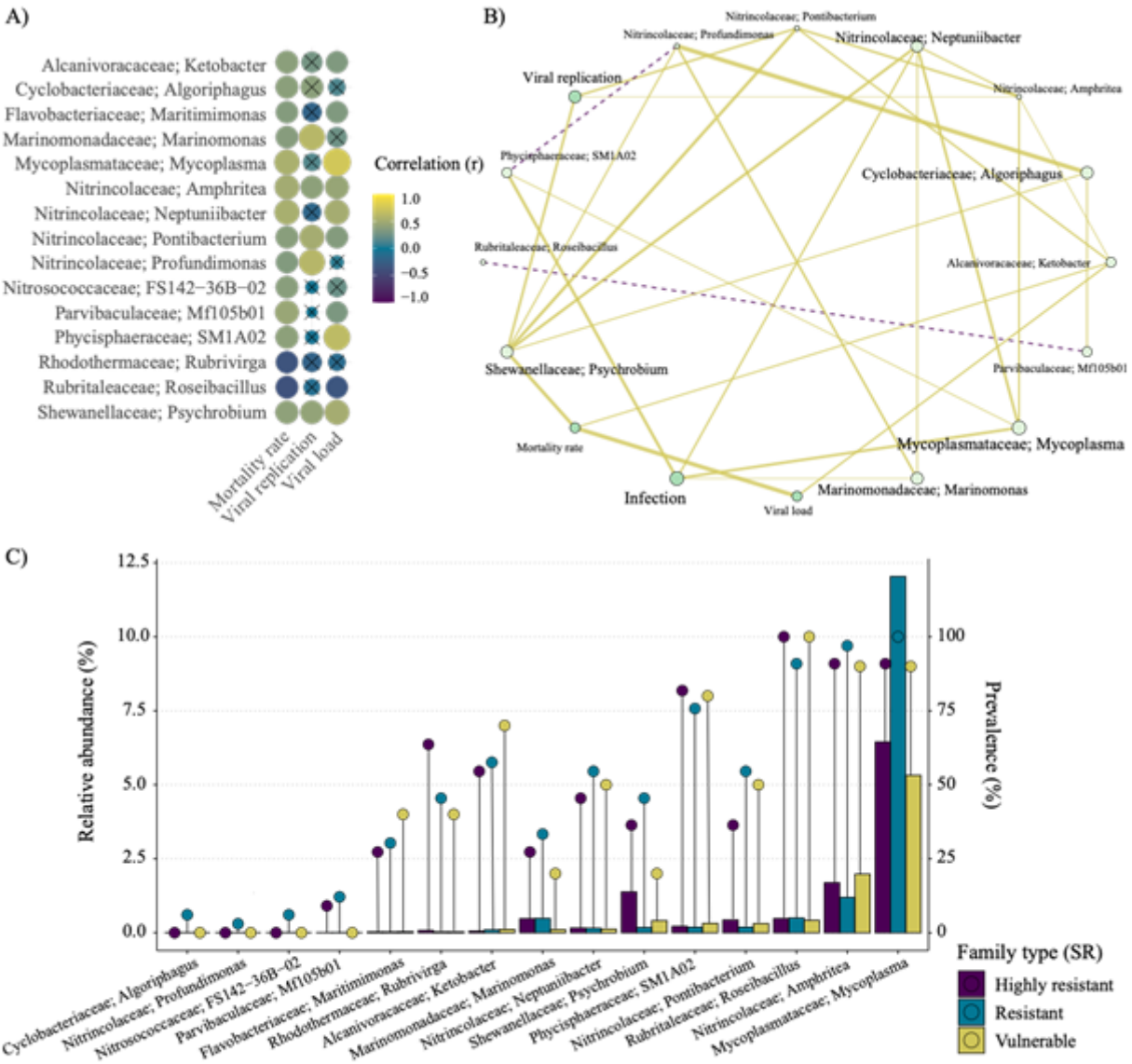

Figure 8

(A) **Pearson correlations of centered-log transformed genera abundance with mortality rate, ORF and viral load, (B) network associations between these bacteria and with mortality rate, viral replication, viral load and treatment and (C) relative abundance (bars) and prevalence (lollipops) of the identified genera per family type (SR).** Only correlations with absolute value > 0.25 are shown, with strength of correlation proportional to line width and positive and negative associations displayed in pale green and in dark blue, respectively. The size of variables (points and text) is proportional to the number of significant associations they have with other variables.

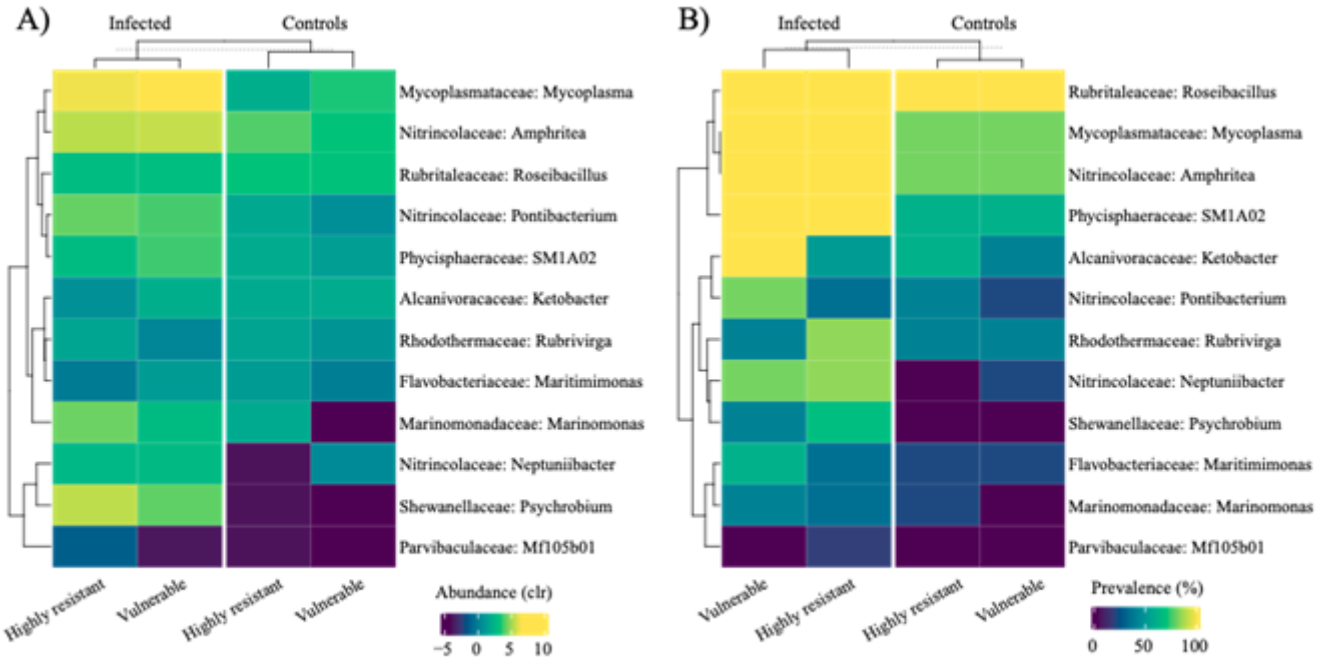

Figure 9

Microbiota relative abundance (A) and prevalence (B) between vulnerable and highly resistant families at genus level. Only genera with a prevalence above 30% and among the 30 most abundant are displayed

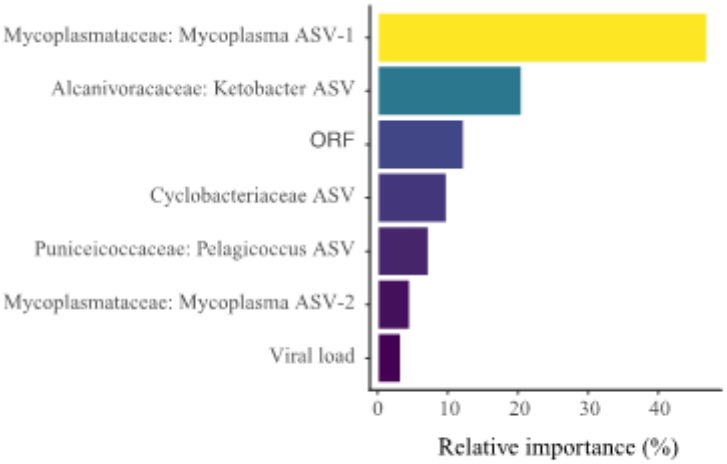

Figure 10

Relative importance of variables selected by a Random Forest analysis to predict mortality rate.

Supplementary Files

This is a list of supplementary files associated with this preprint. Click to download.

- SupplementaryMaterial.docx